

Short Communication

Hybrid carboxymethyl kappa-carrageenan/carboxymethyl cellulose- based biopolymer electrolytes for dye-sensitized solar cell application

S. Rudhziah^{1*}, M. S. A. Rani^{2*}, R.H.Y. Subban^{3,4}, A. Ahmad⁵, N. S. Mohamed⁶, M. R. M. Huzaiifah^{7*}

¹ Centre of Foundation Studies, Universiti Teknologi MARA, Cawangan Selangor, Kampus Dengkil 43800 Dengkil, Selangor, Malaysia.

² School of Materials and Mineral Resources Engineering, Universiti Sains Malaysia, 14300 Nibong Tebal, Pulau Pinang, Malaysia

³ Fakulti Sains Gunaan, Universiti Teknologi MARA, 40450 Shah Alam, Selangor, Malaysia.

⁴ Institut Sains, Universiti Teknologi MARA, 40450 Shah Alam, Selangor, Malaysia.

⁵ School of Chemical Science and Food Technology, Universiti Kebangsaan Malaysia, 43600 Bangi, Malaysia.

⁶ Centre for Foundation Studies in Science, University of Malaya, 50603 Kuala Lumpur, Malaysia

⁷ Department of Crop Science, Faculty of Agricultural Science and Forestry, Universiti Putra Malaysia Bintulu Campus, 97000 Bintulu, Sarawak.

*E-mail: rudhziah@uitm.edu.my ; iker.asmal55@gmail.com ; muhammadhuzaiifah@upm.edu.my

Received: 23 March 2021 / Accepted: 29 August 2021 / Published: 6 December 2021

Natural biopolymers have recently attracted a lot of attention for the development of new polymer electrolytes due to their environmental friendliness, nontoxicity, and abundance in nature. Biopolymer electrolytes based on carboxymethyl kappa-carrageenan/carboxymethyl cellulose incorporated with sodium iodide were prepared and their structural and electrochemical stability were investigated using electrochemical impedance spectroscopy, Fourier transform infrared spectroscopy, transference number measurement, and linear sweep voltammetry. The film containing 30 wt% sodium iodide had the highest ionic conductivity and the highest relative number of charge carriers at room temperature. The relative number of charge carriers for each prepared electrolyte film in this study increased with salt concentration, according to Barker's electrolyte dissociation theory. The highest conducting electrolyte and the lowest salt concentration electrolyte films were used to fabricate and characterise dye-sensitized solar cell (DSSC). These DSSCs responded well to a light intensity of 100 mW cm⁻².

Keywords: Polymer blend; electrolytes; carboxymethyl kappa-carrageenan; carboxymethyl cellulose; sodium iodide.

1. INTRODUCTION

Nowadays, bio-based polymers derived from polysaccharides are gaining attention due to rising environment concerns, as well as rising costs and dwindling supplies of fossil fuels. It is predicted that biopolymers will be one of the primary important renewable energy resources that will provide major raw materials for the advancement of industry in the future [1-3]. Biodegradable polymers have been extensively researched in order to replace conventional non-degradable or incompletely degrading synthetic biopolymers in the development of environmentally friendly polymer electrolytes. Furthermore, most biopolymers exhibit extensive hydrogen bonding, implying that these polymers are more conductive than those with fewer hydrogen bond [4]. As a result, considerable effort has been expended in developing biopolymer electrolytes based on natural polymers such as starch [5, 6], cellulose [7-9], chitosan [10, 11], agar [12, 13] and carrageenan [14, 15].

The dye-sensitized solar cell (DSSC) is one of the most promising methods of solar energy conversion, and it has received a lot of attention since its invention by Grätzel and colleagues in 1991 [16]. The operating principle of this third-generation solar cell is very similar to that of natural plant photosynthesis. This technology is very appealing due to its ease of fabrication, low raw material costs, processing methods using simple and inexpensive equipment, use of environmentally friendly materials, and the ability to fabricate flexible solar cells [17]. Until now, DSSCs with liquid electrolytes have demonstrated the best photovoltaic performance. However, there are some issues with DSSCs liquid electrolytes, such as the volatility of the organic solvent in the electrolytes, evaporation risks, and solvent leakage [18, 19]. As a result, solid-state DSSCs employing solid polymer electrolytes based on biopolymers appear to be a novel alternative that should be investigated in order to replace liquid state DSSCs [20, 21].

In this study, biobased polymers, carboxymethyl kappa-carrageenan (CMKC) and carboxymethyl cellulose (CMCE) were incorporated with sodium iodide as a doping salt to develop biopolymer blend electrolyte (BBE). The chemical interactions, electrical and electrochemical characterizations were investigated. To the best of the author's knowledge, no research on biobased carboxymethyl polymer blend electrolytes doped with sodium iodide and their potential application in DSSC has been published. It is worth looking into the properties of biobased carboxymethyl polymer blend electrolytes and their potential in DSSC.

2. METHOD OF RESEARCH

2.1. Preparation of BBE films

The BBE based CMKC/CMCE were prepared using the solution cast technique. CMKC was synthesized from *k*-carrageenan while CMCE was obtained from kenaf bast fiber based on our previous publication [22]. 1 g of CMKC/ CMCE was dissolved in 1% of acetic acid and stirred continuously for 24 h at 40 °C. Various percentages of NaI were added to the solution. The solutions were further stirred

at room temperature for a few hours to achieve homogenous mixtures. The solutions were then poured into Petri dishes and allowed to dry slowly at room temperature until free-standing films formed.

2.2. Characterization of BBE films

The electrical properties of the BBE films were investigated using a high frequency response analyzer (Solartron 1260) in the frequency range of 10 Hz to 4 MHz with a voltage amplitude of 10 mV at temperatures ranging from 300 to 333 K. The electrochemical impedance data were collected and analyzed at various temperatures. The study on the dielectric behavior can aid in understanding the conductivity behaviour of the electrolytes and so the impedance data were converted into the dielectric constants data, ϵ_r . The following equation was used to calculate the value of ϵ_r :

$$\epsilon_r = \frac{Z_i}{\omega C_o(Z_r^2 + Z_i^2)} \quad (1)$$

where C_o denotes the vacuum capacitance. In order to investigate the interactions of the polymer host and the incorporated NaI, FTIR spectroscopy was performed using a Perkin Elmer Frontier spectrophotometer. The BBE sample was placed on a germanium crystal, and infrared light with a wavenumber range from 4000 to 550 cm^{-1} at a resolution of 1 cm^{-1} was passed through it. In addition, electrochemical stability window and transference number measurement of the BBE films were measured with a Wonatech Zive MP2 multichannel electrochemical instrument. The BBE sample was sandwiched between two stainless steel electrodes for electrochemical stability window measurement, and data were recorded at scan rate of 1 mVs^{-1} . The voltage was applied in the 0 to 5 V range. Meanwhile, Wagner's polarization method was used to calculate the ionic transference number. The BBE is sandwiched between stainless steel electrodes. The polarization current versus time plot was used to calculate the ionic transference number (t_{ion}), which was evaluated from using these equations:

$$t_{\text{ion}} = \frac{I_{\text{initial}} - I_{\text{final}}}{I_{\text{initial}}} \quad (2)$$

$$t_e = \frac{I_{\text{final}}}{I_{\text{initial}}} \quad (3)$$

where t_e is electronic transference number, I_{initial} is the initial current due to the movement of ions and electrons in the applied electric field whereas I_{final} is steady state electron current.

2.3. Fabrication of solid-state DSSC device

The CMKC/CMCE-NaI electrolyte containing of 10 and 30 wt % of NaI were selected as electrolytes in the fabrication of DSSC. The following steps were used to fabricate a solid-state DSSC with an active area of about 1 cm^2 . To make the DSSC photoelectrode, the TiO_2 paste was spread on

FTO conducting glass with a doctor blade technique, then sintering at 450 °C for 30 min. This electrode was then immersed in the dye N719 solution for 24 h. Meanwhile, the platinum FTO glass counter electrode was prepared by brush painting and heating at 450 °C for 30 min. The BBE was then doped with 0.02 M of I₂ for redox couple formation in DSSC. This electrolyte solution was poured onto a TiO₂/dye photoelectrode and heated to 50 °C to form a film. Following that, the TiO₂/dye photoelectrode with electrolyte film was combined with a platinum counter electrode. The photocurrent density-voltage (J-V) characteristics of the DSSCs were used to investigate their performance. The data were collected using Wonatech Zive MP2 multichannel electrochemical workstation under white light illumination (100 mW cm⁻²).

3. RESULTS AND DISCUSSION

3.1. Room temperature conductivity analysis

Table 1 shows the average room temperature conductivity of biopolymer electrolytes with various NaI concentration. The ionic conductivity value increased gradually with increase in salt concentration from $(3.25 \pm 0.25) \times 10^{-4} \text{ S cm}^{-1}$ to $(4.55 \pm 0.08) \times 10^{-3} \text{ S cm}^{-1}$. The CMKC/CMCE BBE system with 30 wt % NaI has the highest ionic conductivity. The increase in ionic conductivity with increasing salt concentration is attributed to an increase in the charge carrier concentration [23, 24]. The ionic conductivity of electrolytes is given as:

$$\sigma = nq\mu \quad (4)$$

where n is the mobile charge carrier density, q is the ion charge and μ is the charge carrier mobility. As a result, any increase in n or μ leads to an increase in conductivity. Barker's electrolyte dissociation theory states that [25]:

$$n = n_o \exp\left(-\frac{U_o}{2\epsilon\kappa_B T}\right) \quad (5)$$

where U_o is the NaI dissociation energy, κ_B is the Boltzmann constant, ϵ is the dielectric constant of the electrolyte system at the selected frequency and T is the sample temperature. The dissociation energy values for each NaI concentration in this study was taken from the book entitled The Strengths of Chemical Bonds, 1958. The relative number of charge carriers (n/n_o) for each film prepared was calculated using equation 5, and the results are tabulated in Table 1. The n/n_o ratio increased as NaI concentration increased. The highest n/n_o was observed in the CMKC/CMCE BBE film with the highest ionic conductivity in the system. This confirms that the number of charge carriers governs the conductivity of the CMKC/CMCE BBE film.

Table 1. Conductivity, relative number of charge carriers and activation energy for the CMKC/CMCE BBE films at room temperature.

NaI concentration (wt %)	Conductivity, σ (S cm ⁻¹)	n/n_o	E_a (eV)
0	3.25×10^{-4}	-	0.015
10	1.59×10^{-3}	0.984	0.008
20	2.94×10^{-3}	0.993	0.018
30	4.55×10^{-3}	0.997	0.022

3.2. Dielectric study

Fig. 1 (A) depicts the plots of dielectric constant variation with NaI concentration for all BBE films at selected frequencies ranging from 10 Hz to 40 kHz at room temperature. Low frequency has the highest dielectric constant. At low frequency, the period of the applied electric field is long, and ions accumulate at the electrode/electrolyte interface. The dielectric constant for each frequency is observed to increase as NaI concentration increases. The increase in dielectric constant with NaI concentration reflects an increase in charge carrier number [26, 27]. This observation is consistent with the n/n_o results in Table 1. As a result, there is strong evidence that the number of charge carriers has an effect on conductivity.

3.3. Various temperature conductivity studies

To investigate the conductivity-temperature behaviour of the BBE films, the conductivity of electrolyte films was measured at various temperatures ranging from 303 to 333 K (**Fig. 1 (B)**). The conductivity is observed to increase with temperature. All temperature dependence of conductivity plots show no abrupt temperature jump, indicating that the BBE is amorphous [28]. This result demonstrated that ionic conduction in BBE follows the Vogel-Tammann-Fulcher (VTF) relationship which is expressed as:

$$\sigma = \sigma_o T^{-\frac{1}{2}} \exp \left(\frac{-E_a / \kappa_B}{(T - T_o)} \right) \quad (6)$$

where σ_o is the pre-exponential factor, E_a denotes the activation energy, κ_B is the Boltzmann constant, T denotes the absolute temperature and T_o is the ideal vitreous transition temperature at which the polymer segments begin to move. T_o is also the reference temperature taken as the glass transition temperature, T_g . The slope of linear VTF plot for each BBE systems resulted in activation energy value

(Table 1). The value of E_a for CMKC/CMCE BBE systems is smaller than 0.05 eV. This behaviour indicates that the BBE has favourable properties for use in electrochemical devices.

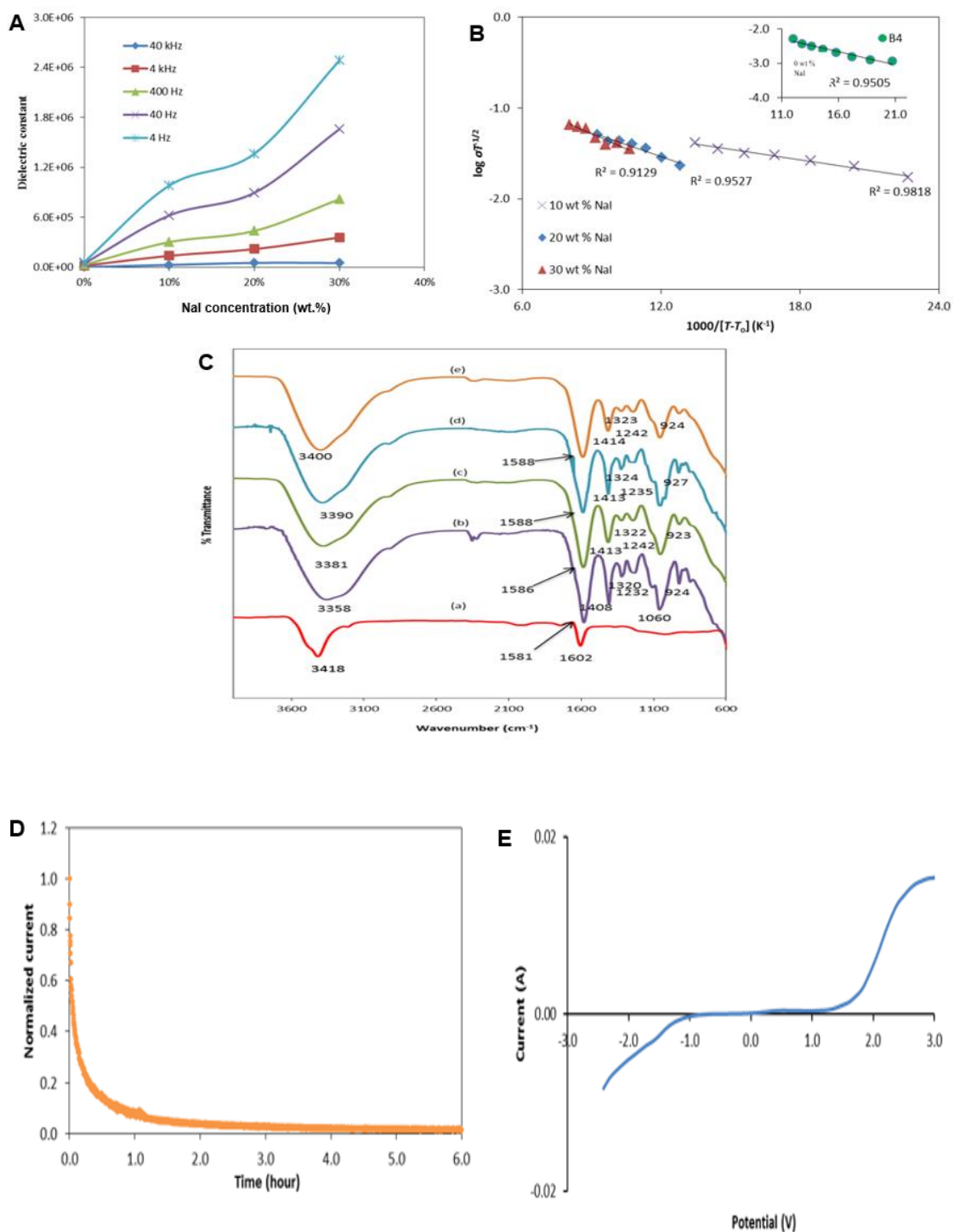


Figure 1. (A) Real part of dielectric constant versus salt concentrations at various frequencies for CMKC/CMCE-NaI films, (B) VTF plots for CMKC/CMCE-NaI films, (C) FTIR spectra for (a) NaI and CMKC/CMCE-NaI films containing (b) 0, (c) 10, (d) 20 and (e) 30 wt % of NaI, (D) Polarization current versus time for the CMKC/CMCE BBE film containing 30 wt % of NaI, (E) LSV curve for CMKC/CMCE-30 wt % NaI film.

3.4. Interaction analysis

FTIR spectra were collected and analysed to investigate the interactions of CMKC/CMCE-NaI complexes. The recorded FTIR spectra of CMKC/CMCE with various concentrations of NaI in the spectral region of 600 to 4000 cm^{-1} (**Fig. 1 (C)**). The bands at 3358, 1581, 1408, 1320, 1232 and 924 cm^{-1} correspond to O-H stretching, COO^- asymmetrical of carboxylate anion, COO^- symmetric stretching, $-\text{CH}_2$ scissoring, $\text{O}=\text{S}=\text{O}$ symmetric vibration and C-O-C stretching of CMKC/CMCE (0 wt% salt) [29, 30]. After addition of NaI, the bands in the CMKC/CMCE BBE (0 wt%) are shifted to higher wavenumbers. The 3358, 1581, 1408, 1320, 1232 and 924 cm^{-1} wavenumbers are detected at higher wavenumbers in the BBE system. Upon NaI addition, the intensity of these bands decreases. This could be due to Na^+ ions interactions with the carboxy and hydroxyl group of the polymer host [7, 31, 32]. These changes suggest a biopolymers-NaI interaction in the CMKC/CMCE BBE.

3.5. Chronoamperometry and voltammetry analysis

The ionic transference number for the highest ionic conducting film was determined using the DC polarisation method to determine the fraction of conductivity due to ion movement. **Fig. 1(D)** illustrates the transference number measurement result of polymer electrolytes based on CMKC/CMCE-NaI. The ionic transference number value of the BBE containing 30 wt% of NaI is found to be ~ 0.99 . Meanwhile, the electrochemical stability window of the BBE film is up to 1.0 V (**Fig. 1(E)**). This demonstrated that the CMKC/CMCE BBE film is electrochemically stable enough for use in DSSCs [7, 33].

3.6. J-V performance

Fig. 2 depicts the photocurrent density-voltage curves of DSSCs made with BBE films containing 10 wt % and 30 wt % NaI. The concentration of iodide has a positive effect on both conductivity and J_{sc} values. The BBE film of 10 wt% NaI shows a lower J_{sc} and higher V_{oc} (as displayed in Table 2). The lower J_{sc} value of this cell is due to its lower ionic conductivity. It has a higher ion migration resistance, which reduces the supply of I_3^- to the Pt counter-electrode. This resulted in I_3^- depletion as well as a delay in the kinetics of dye regeneration, lowering the J_{sc} value. However, as the concentration of NaI increased, the J_{sc} value also increased. The higher value of J_{sc} is exhibited by the BBE-30 wt% NaI which is due to its higher ionic conductivity. The higher conductivity resulted in a faster regeneration of the dye-sensitizer from its oxidized state to its original state at the dye-electrolyte interface [19, 34, 35]. The highest conducting CMKC/CMCE-NaI photoelectrochemical cell demonstrated the best performance of 0.16 %. Based on the findings, this BBE system has promising properties for DSSC applications.

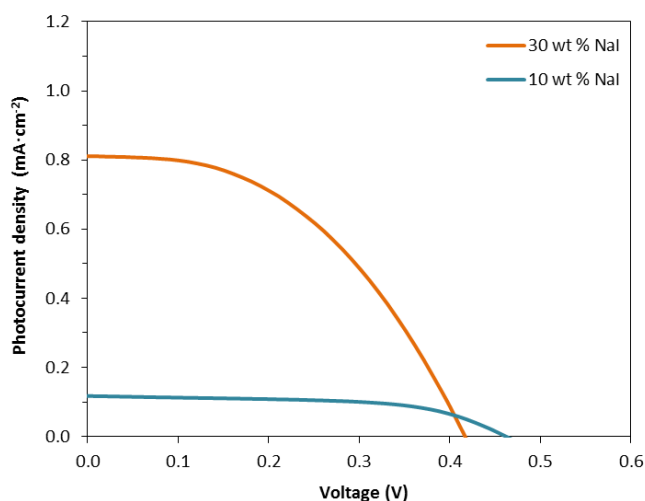


Figure 2. Photocurrent density-voltage for FTO-TiO₂/ BBE /I₂/Pt-FTO cell.

Table 2. J-V performance.

NaI concentration (wt%)	V _{oc} (V)	J _{sc} (mA cm ⁻²)	ff	η%
10	0.47	0.12	0.57	0.03
30	0.43	0.81	0.44	0.16

4. CONCLUSION

BBE based CMKC/CMCE-NaI were successfully prepared and characterized. The following conclusions have been obtained from the results:

- The conductivity of CMKC/CMCE was improved from $(3.25 \pm 0.25) \times 10^{-4} \text{ S cm}^{-1}$ to $(4.55 \pm 0.08) \times 10^{-3} \text{ S cm}^{-1}$ with the addition of 30 wt% of NaI.
- Temperature dependence analysis demonstrated that ionic conduction in BBE follows the Vogel-Tammann-Fulcher (VTF) rule.
- The complexation between CMKC/CMCE and NaI was confirmed by the FTIR analysis.
- The LSV curve showed that this electrolyte was electrochemically stable up to $\sim 1.0 \text{ V}$ and the ionic transference number value of the BBE containing 30 wt% of NaI was found to be ~ 0.99 .
- The DSSCs using CMKC/CMCE-30 wt% NaI electrolytes has an efficiency of 0.16%.

CONFLICTS OF INTEREST

The authors declare there are no conflict of interest.

ACKNOWLEDGEMENTS

The authors gratefully acknowledge financial supports from Universiti Teknologi MARA, Fundamental Research Grant Scheme (FRGS) [File No.: 600-IRMI/FRGS 5/3 (342/2019)] and Ministry of Higher of Higher Education (MOHE) provided for this work.

References

1. N.M. Nurazzi, M.R.M. Asyraf, M. Rayung, M.N.F. Norrrahim, S.S. Shazleen, M. Rani, A.R. Shafi, H.A. Aisyah, M.H.M. Radzi, F.A. Sabaruddin and R.A. Ilyas, *Polymers*, 13 (2021) 2710.
2. M.N.F. Norrrahim, R.A. Ilyas, N.M. Nurazzi, M.S.A. Rani, M.S.N. Atikah, and S.S. Shazleen, *Applied Science and Engineering Progress*, (2021) doi: 10.14416/j.asep.2021.07.004
3. M.H. Sainorudin, N.A. Abdullah, M.S.A. Rani, M. Mohammad, M. Mahizan, N. Shadan, N.H. Abd Kadir, Z. Yaakob, A. El-Denglawey, and M. Alam, *Nanotechnology Reviews*, 10 (2021) 793-806.
4. V.L. Finkenstadt, *Applied microbiology and biotechnology*, 67 (2005) 735-745.
5. M. Yadav, G. Nautiyal, A. Verma, M. Kumar, T. Tiwari, and N. Srivastava, *Ionics*, 25 (2019) 2693-2700.
6. C.-W. Liew, S. Ramesh, K. Ramesh, and A.K. Arof, *Journal of Solid State Electrochemistry*, 16 (2012) 1869-1875.
7. M.S.A. Rani, M. Mohammad, M.S. Sua'it, A. Ahmad, and N.S. Mohamed, *Polymer Bulletin*, 78 (2021) 5355-5377.
8. K.H. Kamarudin, M.S.A. Rani, and M.I.N. Isa, *American-Eurasian Journal of Sustainable Agriculture*, (2015) 8-15.
9. M.S.A. Rani, N.H. Hassan, A. Ahmad, H. Kaddami, and N.S. Mohamed, *Ionics*, 22 (2016) 1855-1864.
10. M.S.A. Rani, N.S. Mohamed, and M.I.N. Isa. *Characterization of proton conducting carboxymethyl cellulose/chitosan dual-blend based biopolymer electrolytes*. in *Materials Science Forum*. 2016. Trans Tech Publ.
11. S.B. Aziz, M. Brza, H. Hamsan, M. Kadir, and R.T. Abdulwahid, *Polymer Bulletin*, 78 (2021) 3149-3167.
12. S. Selvalakshmi, T. Mathavan, S. Selvasekarapandian, and M. Premalatha, *Journal of Solid State Electrochemistry*, 23 (2019) 1727-1737.
13. S. Selvalakshmi, T. Mathavan, S. Selvasekarapandian, and M. Premalatha, *Ionics*, 24 (2018) 2209-2217.
14. V. Moniha, M. Alagar, S. Selvasekarapandian, B. Sundaresan, and R. Hemalatha, *Materials Today: Proceedings*, 8 (2019) 449-455.
15. P. Sangeetha, T. Selvakumari, S. Selvasekarapandian, S. Srikumar, R. Manjuladevi, and M. Mahalakshmi, *Ionics*, 26 (2020) 233-244.
16. B. O'regan and M. Grätzel, *Nature*, 353 (1991) 737-740.
17. S. Rudhzhiah, A. Ahmad, I. Ahmad, and N.S. Mohamed, *Electrochimica Acta*, 175 (2015) 162-168.
18. F. Bella, C. Gerbaldi, C. Barolo, and M. Grätzel, *Chemical Society Reviews*, 44 (2015) 3431-3473.
19. N.A. Dzulkurnain, M.S.A. Rani, A. Ahmad, and N.S. Mohamed, *Ionics*, 24 (2018) 269-276.
20. N.A. Rahman, S.A. Hanifah, N.N. Mobarak, A. Ahmad, N.A. Ludin, F. Bella, and M.S. Su'ait, *Polymer*, (2021) 124092.
21. S. Galliano, F. Bella, M. Bonomo, F. Giordano, M. Grätzel, G. Viscardi, A. Hagfeldt, C. Gerbaldi, and C. Barolo, *Solar Rrl*, (2021) 2000823.
22. S. Rudhzhiah, M.S.A. Rani, A. Ahmad, N.S. Mohamed, and H. Kaddami, *Industrial Crops and Products*, 72 (2015) 133-141.
23. M. Singh, V.K. Singh, K. Surana, B. Bhattacharya, P.K. Singh, and H.-W. Rhee, *Journal of Industrial and Engineering Chemistry*, 19 (2013) 819-822.
24. V. Aravindan and P. Vickraman, *Ionics*, 13 (2007) 277-280.
25. R. Barker Jr and C.R. Thomas, *Journal of Applied Physics*, 35 (1964) 3203-3215.
26. M. Hema, S. Selvasekerapandian, A. Sakunthala, D. Arunkumar, and H. Nithya, *Physica B: Condensed Matter*, 403 (2008) 2740-2747.
27. M.S.A. Rani, A. Ahmad, and N.S. Mohamed, *Polymer Bulletin*, 75 (2018) 5061-5074.
28. R. Nadimicherla, R. Kalla, R. Muchakayala, and X. Guo, *Solid State Ionics*, 278 (2015) 260-267.

29. C.L. Tien, M. Millette, M.A. Mateescu, and M. Lacroix, *Biotechnology and applied biochemistry*, 39 (2004) 347-354.
30. C.T. Aranilla, N. Nagasawa, A. Bayquen, and A.D. Rosa, *Carbohydrate polymers*, 87 (2012) 1810-1816.
31. M.S.A. Rani, N.S. Isa, M.H. Sainorudin, N.A. Abdullah, M. Mohammad, N. Asim, H. Razali, and M.A. Ibrahim, *Int. J. Electrochem. Sci.*, 16 (2021) 210354.
32. M.S.A. Rani, S. Rudhzhiah, A. Ahmad, and N.S. Mohamed, *Polymers*, 6 (2014) 2371-2385.
33. M.S.A. Rani, M.H. Sainorudin, N. Asim, and M. Mohammad, *Int. J. Electrochem. Sci.*, 15 (2020) 11833-11844.
34. M.Y.A. Rahman, A. Ahmad, A.A. Umar, R. Taslim, M.S. Su'ait, and M. Salleh, *Ionics*, 20 (2014) 1201-1205.
35. M.S.A. Rani, N.A. Abdullah, M.H. Sainorudin, M. Mohammad, and S. Ibrahim, *Materials Advances*, (2021) (in press).

© 2022 The Authors. Published by ESG (www.electrochemsci.org). This article is an open access article distributed under the terms and conditions of the Creative Commons Attribution license (<http://creativecommons.org/licenses/by/4.0/>).